THE ASTROPHYSICAL JOURNAL, 306:183–198, 1986 July 1

FOURIER COEFFICIENTS OF VARIABLE STARS

R. F. STELLINGWERF AND M. DONOHOE
Mission Research Corporation, Alburquerque, New Mexico
Received 1985 October 9; accepted 1985 December 23

ABSTRACT

Since the early days of observational astronomy, the technique of Fourier decomposition of the light curves of variable stars (harmonic analysis) has been used to quantify the light curve shape. Usually, the most reasonable approach when dealing with observations is a least-squares fit to the data, which yields a set of Fourier phases and amplitudes whose number is determined by the quality of the data set, generally 5–15 parameters. An interesting question is whether these parameters can be related to physical characteristics of the star, such as mass, gravity, composition, etc. Here we compute the Fourier parameters of velocity curves of adiabatic one-zone pulsation models in an effort to identify the expected properties of this simple case. Two parameters are varied: the thickness of the pulsating layer (determined by the structure of the star), and the amplitude of the pulsation. We find Fourier amplitudes that are primarily functions of the skewness of the velocity curves and vary in a fashion consistent with the behavior of observed stars. The phases, however, tend to vary discontinuously as the parameters are varied, an effect seen only rarely in the observations. It is shown that the pattern of phases for different harmonics is more important than the actual values, and that these patterns can be found in observations of RR Lyrae stars and Cepheids. This model cannot, however, reproduce the large phase shifts seen in observed stars of differing periods.

Subject headings: numerical methods — stars: Cepheids — stars: pulsation — stars: RR Lyrae — stars: variables

I. INTRODUCTION

The light curve of a variable star is its most easily obtained observational characteristic. It is now well known that the general shape of the curve as well as the phasing and prominence of definite features change in a regular way as parameters such as period, luminosity, and variable type vary. The characterization of the RR Lyrae types a, b, and c (Bailey 1902) and the "bump" progression in Cepheids (Hertzsprung 1926) represent phenomena in this class.

Unfortunately, the "light curve shape" is a qualitative notion and needs to be described in quantitative terms to enable reliable classification and analysis. Derivation of Fourier coefficients is one approach applied to Cepheids by Kukarkin and Parenago (1937), and for a variety of types of stars by Payne-Gaposchkin (1947, hereafter PG47). In these analyses we find "a striking run with period, both of the relative amplitudes of Fourier components, and of the phase relations between components" (PG47). This supports the idea that a classification scheme based on such an analysis could be useful.

Fourier fitting to construct smooth fits to data is, of course, a widely used technique (see, e.g., Schaltenbrand and Tamman 1971). The order (highest harmonic) of a useful fit is determined by the largest gap in the phase coverage of the light curve. For most stars and data sets, an order 5 fit works well, yielding a set of 11 Fourier coefficients, including the mean magnitude.

Interest in this technique has recently been reawakened by Simon and Lee (1981), who analyzed classical Cepheid light curves and attributed a break in the Fourier coefficients found at a period of 10 days to a resonance phenomenon responsible for the Hertzsprung sequence of light curve "bumps." Subsequent papers by Simon and Teays (1982), Simon and Davis (1983), Simon and Moffet (1985, hereafter SM85) and Simon (1985) have enlarged the scope of this study to include field RR Lyrae stars and comparison with calculated models. In general it is found that, in agreement with the earlier work, the Fourier amplitudes and phases are reasonably well defined and can be used to distinguish between different types of stars. Recent theoretical work by Klapp, Goupil, and Buchler (1985), and Buchler and Kovacs (1985) suggests that multimode resonances play a major role in determining the light curve structure.

A valuable recent addition to the data base has been provided by Petersen (1984), who reanalyzed the mean light curves given by Martin (1983) of the variables in the globular cluster ω Cen (also analyzed by PG47) and showed that well-defined values and trends in the Fourier parameters were present through the seventh harmonic for this data set. These RR Lyrae stars show variation in their Fourier phases similar to, but not as strong as, those found in the Cepheid studies.

It is clear that the observed changes in the shape of the light curve are directly related to structural and dynamic properties of the star. Petersen (1985) outlines a program whereby a detailed comparison of Fourier analyses of hydrodynamic models with those of observed stars could yield information about the structure and evolutionary status of the stars and perhaps resolve several outstanding problems with our understanding of these objects (e.g., the cause of the bump progression, the stellar masses, the cause of mixed-mode stars, and the mechanism of mode selection; see Madore 1985 for discussions of current problems in this field). Unfortunately, our understanding of the nature of the Fourier parameters is far from adequate to allow such a program at the present time. The comparisons with models that have been made work well for some of the low-order coefficients but fail for others (Simon 1985). It is not known what values of the Fourier parameters to expect, or what it means to be "close" to an observed case: small changes in the light-curve shape can cause large changes

in the Fourier coefficients, particularly in the higher orders. Finally, it is not known how many Fourier terms are needed to obtain useful results. It is clear from the analysis of PG47 that in most cases all the Fourier amplitudes and phases are highly correlated and may all be determined by only one or two properties of the pulsating star.

In this paper we present the results of a study intended to lay some groundwork to begin to answer these questions. We present the results of Fourier analyses of the variation of a very simple model: the adiabatic pulsations of a single homogeneous layer of a sphere with fixed lower boundary. In this nonlinear problem there are only two adjustable parameters: the thickness of the layer (varies from the entire sphere to an infinitesimally thin layer at the surface), and the initial amplitude of the oscillation, both directly related to actual stars. We study the changes in the fitting coefficients as these parameters are varied and attempt to relate the results to the analyses of actual stars. In this way we can hope to isolate the effects of stellar structure and amplitude. Effects seen in the stars, but not in this model, must be caused by more complicated phenomena, such as multimode processes.

II. METHOD

a) *Fourier Analysis*

The technique used for the Fourier analysis is identical to that described by Petersen (1984): least-squares fitting of a given number of Fourier terms to a general data set. The data to be fitted are given by $(x_j, t_j), j = 1, M$. The fitting function is written

$$m(t) = m_0 + \sum_{k=1}^{N} [a_k \sin(k\omega t) + b_k \cos(k\omega t)] , \quad (1)$$

where m_0 is the mean of the data, N is the order of the fit, and ω is 2π/period. The least-squares normal equations are given by the derivatives of

$$S(m_0, a_k, b_k) = \sum_{j=1}^{M} [m(t_j) - x_j]^2 , \quad (2)$$

They form a linear system in the unknowns m_0, a_k, and b_k (assuming that the period of pulsation is known) and are easily solved on a microcomputer.

The results are then converted to the form

$$m(t) = m_0 + \sum_{k=1}^{N} [H_k \cos(k\omega t + \phi_k)] , \quad (3)$$

and the quantities

$$R_k = H_k/H_1 \quad (4)$$

and

$$\phi_{k1} = \phi_k - k\phi_1 \quad (5)$$

are computed. These are the dimensionless amplitude ratio of the harmonics, and the phase difference between harmonics and the fundamental. Note that equation (3) defines each phase on its own scale, so the phase of the kth harmonic runs from 0 to $2\pi k$ in one period. Equation (5) gives the phase difference, on this scale, of the peak of the fundamental mode and the kth harmonic peak just preceding it. Each of these phase differences lie in the range $0 \rightarrow 2\pi$. To convert to actual phase (eq. [6]), divide equation (5) by k.

Once the fit is obtained, we find the "pulsation phase"

$$f = \text{fractional part of } (t/\text{period}) \quad (6)$$

of the maximum and minimum values of the fit (f_{max}, f_{min}) and define

$$\text{amplitude} = m(f_{max}) - m(f_{min}) \quad (7)$$

and

$$\text{skewness} = (1 - f_{max} + f_{min})/(f_{max} - f_{min}) . \quad (8)$$

This definition applies to the orientation given below. The skewness is defined as the ratio of the phase length of the "descending branch" to that of the "rising branch" and is generally greater than unity for observed stars.

The routine used for this analysis was tested on ω Cen data from Petersen (1984). Then two additional tests were run on the smooth data derived from the model described below: (1) the least-squares fit on a smooth curve defined by over 200 data points was compared to Fourier coefficients computed directly from the integral formulae—the results agreed exactly; and (2) fits of order 1–10 were run on the same data—coefficients of the lower order fits agreed exactly with those found for higher orders.

b) *One-Zone Model*

The pulsation model considered here is a simple version of the model derived by Stellingwerf (1972), based on the one-zone model of Baker (1966). Consider a spherical homogeneous adiabatic shell of outer radius r and inner radius r_c. Its inner surface is fixed, while its outer surface is free to move but has an equilibrium position, r_0. Defining $X = r/r_0$, we write

$$\frac{\rho}{\rho_0} = X^{-m} , \quad (9)$$

$$\frac{P}{P_0} = \left(\frac{\rho}{\rho_0}\right)^{\Gamma_1} = X^{-m\Gamma_1} , \quad (10)$$

$$\frac{T}{T_0} = X^{-m(\Gamma_1 - 1)} , \quad (11)$$

where

$$m = \frac{3}{1 - (r_c/r_0)^3} , \quad (12)$$

$$\Gamma_1 = \left(\frac{\partial \ln P}{\partial \ln \rho}\right)_S , \quad (13)$$

for the density, pressure, and temperature in the shell as functions of the surface displacement, assuming perfect gas. We define

$$q = m\Gamma_1 - 2 \approx 9 \quad (14)$$

and take as the unit of time the free-fall time:

$$\tau = t/t_{ff} , \quad (15)$$

$$t_{ff} = \left(\frac{GM}{r_0^3}\right)^{-1/2} \quad (16)$$

With these definitions, the momentum equation for the shell can be written:

$$\frac{d^2X}{d\tau^2} = \frac{1}{X^q} - \frac{1}{X^2} , \quad (17)$$

where zero external pressure is assumed.

We adopt a standard case with $\Gamma_1 = 5/3$ and take "m" as a

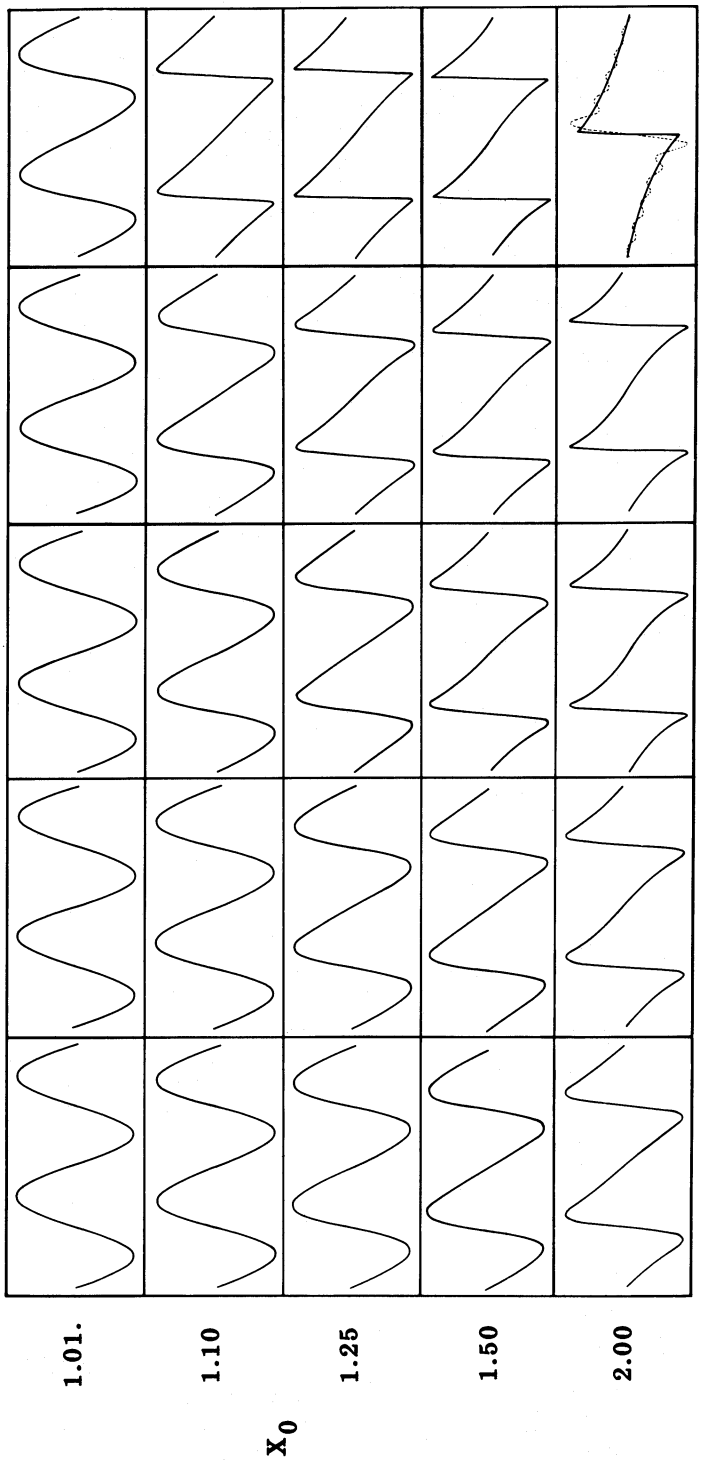

FIG. 1.—Velocity vs. phase, normalized to unity, for the cases described in Table 1. Here m is a measure of the thickness of the pulsating shell and X_0 is the starting amplitude. The dashed line in the lower right case is the Fourier fit.

constant to be specified. Interpretation of the cases in terms of shell thickness is given by equation (12). Once m is chosen, q is given by equation (14), and equation (17) is fully specified. An integration run consists of choosing the starting value of X, X_0; setting the velocity $\dot{X}$ equal to zero; and proceeding with a fourth-order Runge-Kutta integration for several periods. With proper choice of time step, the integration reproduces exactly each period—as expected for an adiabatic oscillation.

The linear period for this model is easily shown to be

$$period_0 = 2\pi/(m\Gamma_1 - 4)^{1/2} . \quad (18)$$

At finite amplitude, nonlinear effects cause appreciable lengthening of the period. This effect is much stronger in this simple case than in actual stars, because several sources of nonlinear effects have been omitted (primarily the choice of constant m and the assumption of homogeneity in the shell), thus forcing the use of higher amplitudes to achieve a similar nonlinear effect. We emphasize that the periods found here are not to be compared with stellar periods, for in stars the period is determined primarily by the free-fall time, and this effect is normalized out of the present equation.

III. SURVEY

A set of 25 models was computed at five values of m: 3, 5, 10, 20, and 100, and at five values of the initial radius X_0: 1.01, 1.10, 1.25, 1.50, and 2.00. Normally two periods were run of each case, with the integration step chosen to give about 100 steps per period. The resulting velocity curve shapes are shown in Figure 1, normalized to constant period and amplitude. Two additional cases were run to represent the extremes: the case $m = 3$, $X_0 = 1.0001$, and the case of a pure "sawtooth" variation—linear decrease and abrupt increase at phase 0.5.

Order 10 Fourier fits were computed for all these cases, with the orientation and phase chosen exactly as shown in Figure 1. The effects of changing these choices are discussed below. Although these results will apply strictly only to the velocity variation, in actual stars the light curve and the velocity curve are generally very similar in shape, and the Fourier parameters are highly correlated (Buchler and Kovacs 1985).

A complete tabulation of the results of these calculations are given in Table 1. "Sigma" is the standard deviation of the fit with respect to the data. Excellent fits were obtained in all cases, with the exception of a few extreme cases in the lower right-hand corner of Figure 1: the most extreme case is shown as a dashed line in Figure 1. Interpretation of these data is given in the next two sections.

IV. TRENDS IN AMPLITUDES

Here we address the systematics of the Fourier amplitudes. In order to detect effects other than those induced by a change in the overall amplitude of the curves, the relative amplitudes R_{k1} (eq. [4]) are usually studied, rather than the raw H_k values.

Simon and Lee (1981) show plots of R_{21} and R_{31} versus period and versus amplitude for Cepheids. The period plot shows complicated behavior, with a dip in these quantities near a period of 10 days. The amplitude plots are much less well defined but do show a rough correlation of R and the Cepheid amplitudes. Examination of Table 1 indicates that the R do vary smoothly with amplitude for each value of m, but this variation is different in the different sequences. Figures 2 and 3 show the variation of R_{21} through R_{91} versus amplitude for all models. Only a very rough correlation can be discerned, similar to the Cepheid case. There is, however, another parameter that does correlate much better, the skewness of the curve.

TABLE 1

FOURIER FIT PARAMETERS

	X_0	m	period	amplitude	skewness	sigma	H_1	R_{21}	R_{31}	R_{41}	R_{51}	R_{61}	R_{71}
1	1.0001	3	6.280E+0	1.979E-4	1.025E+0	1.030E-6	9.917E-5	5.399E-3	2.971E-3	1.990E-3	1.433E-3	1.059E-3	7.828E-4
2	1.01	3	6.350E+0	1.960E-2	1.015E+0	7.399E-6	9.799E-3	1.030E-2	1.305E-4	1.732E-4	1.346E-4	1.109E-4	9.446E-5
3	1.10	3	6.440E+0	1.800E-1	1.300E+0	4.538E-4	8.925E-2	9.330E-2	8.031E-3	1.953E-3	6.375E-4	6.298E-4	5.228E-4
4	1.25	3	6.790E+0	3.960E-1	1.694E+0	3.067E-3	1.902E-1	2.055E-1	4.172E-2	1.295E-2	7.301E-4	2.192E-3	1.172E-3
5	1.50	3	7.600E+0	6.606E-1	2.392E+0	3.761E-3	2.975E-1	3.271E-1	1.164E-1	4.669E-2	1.688E-2	8.126E-3	2.193E-3
6	2.00	3	9.800E+0	9.878E-1	4.157E+0	7.514E-3	3.883E-1	4.677E-1	2.422E-1	1.361E-1	7.602E-2	4.557E-2	2.573E-2
7	1.01	5	3.030E+0	4.083E-2	1.047E+0	1.757E-5	2.041E-2	1.476E-2	5.256E-4	1.893E-4	1.520E-4	1.253E-4	1.069E-4
8	1.10	5	3.120E+0	3.586E-1	1.437E+0	1.817E-4	1.763E-1	1.342E-1	1.955E-2	3.221E-3	3.434E-4	1.896E-4	8.345E-5
9	1.25	5	3.440E+0	7.437E-1	2.071E+0	1.756E-3	3.464E-1	2.721E-1	8.378E-2	2.568E-2	8.997E-3	2.407E-3	1.266E-3
10	1.50	5	4.250E+0	1.153E+0	3.249E+0	4.973E-3	4.779E-1	4.208E-1	1.941E-1	9.591E-2	4.684E-2	2.459E-2	1.186E-2
11	2.00	5	6.280E+0	1.622E+0	6.949E+0	9.281E-3	5.363E-1	5.508E-1	3.402E-1	2.217E-1	1.479E-1	1.008E-1	6.910E-2
12	1.01	10	1.770E+0	6.894E-2	1.034E+0	1.070E-4	3.448E-2	2.671E-2	1.798E-3	6.266E-4	5.110E-4	4.162E-4	3.500E-4
13	1.10	10	1.920E+0	5.472E-1	1.782E+0	1.048E-3	2.616E-1	2.213E-1	5.580E-2	1.361E-2	4.130E-3	6.277E-4	5.580E-4
14	1.25	10	2.400E+0	1.018E+0	3.210E+0	3.392E-3	4.307E-1	4.012E-1	1.791E-1	8.534E-2	4.020E-2	2.024E-2	9.342E-3
15	1.50	10	3.360E+0	1.454E+0	5.999E+0	9.125E-3	5.151E-1	5.169E-1	3.102E-1	1.945E-1	1.271E-1	8.303E-2	5.594E-2
16	2.00	10	5.580E+0	1.990E+0	9.333E+0	4.017E-2	5.242E-1	5.957E-1	4.121E-1	3.045E-1	2.331E-1	1.824E-1	1.447E-1
17	1.01	20	1.160E+0	1.021E-1	1.148E+0	8.401E-4	5.116E-2	4.491E-2	7.243E-3	2.731E-3	2.171E-3	1.646E-3	1.268E-3
18	1.10	20	1.420E+0	6.905E-1	2.550E+0	7.048E-3	3.096E-1	3.322E-1	1.331E-1	5.044E-2	2.315E-2	7.639E-3	4.728E-3
19	1.25	20	2.040E+0	1.157E+0	5.799E+0	9.033E-3	4.331E-1	4.860E-1	2.845E-1	1.738E-1	1.119E-1	7.109E-2	4.729E-2
20	1.50	20	3.080E+0	1.653E+0	8.625E+0	3.467E-2	4.916E-1	5.478E-1	3.675E-1	2.606E-1	1.969E-1	1.487E-1	1.170E-1
21	2.00	20	5.149E+0	2.053E+0	9.300E+0	7.807E-2	5.017E-1	5.930E-1	4.244E-1	3.168E-1	2.610E-1	2.088E-1	1.791E-1
22	1.01	100	5.280E-1	1.995E-1	1.749E+0	8.786E-4	9.604E-2	2.070E-1	5.197E-2	1.117E-2	4.117E-3	1.214E-4	8.992E-4
23	1.10	100	1.080E+0	8.686E-1	7.999E+0	1.153E-2	2.894E-1	5.026E-1	3.195E-1	2.244E-1	1.641E-1	1.238E-1	9.427E-2
24	1.25	100	1.800E+0	1.520E+0	1.099E+1	7.037E-2	3.894E-1	5.474E-1	3.814E-1	2.950E-1	2.419E-1	2.098E-1	1.898E-1
25	1.50	100	2.880E+0	2.107E+0	1.209E+1	1.510E-1	4.548E-1	5.745E-1	4.109E-1	3.292E-1	2.819E-1	2.524E-1	2.343E-1
26	2.00	100	5.109E+0	2.267E+0	1.177E+1	2.147E-1	4.802E-1	6.030E-1	4.338E-1	3.477E-1	2.949E-1	2.558E-1	2.374E-1
27	sawtooth		1.000E+0	1.070E+0	8.999E+0	1.438E-1	3.182E-1	4.995E-1	3.324E-1	2.487E-1	1.984E-1	1.647E-1	1.405E-1

TABLE 1—*Continued*

	X_0	m	R_{81}	R_{91}	R_{101}	ϕ_1	ϕ_2	ϕ_3	ϕ_4	ϕ_5	ϕ_6	ϕ_7	ϕ_8
1	1.0001	3	5.662E-4	3.896E-4	2.417E-4	1.543E+0	1.437E+0	1.351E+0	1.269E+0	1.188E+0	1.108E+0	1.029E+0	9.519E-1
2	1.01	3	8.229E-5	7.296E-5	6.554E-5	1.572E+0≪	4.717E+0	4.782E+0	4.768E+0	4.784E+0	4.799E+0	4.814E+0	4.829E+0
3	1.10	3	4.549E-4	4.007E-4	3.574E-4	1.584E+0	4.739E+0	1.618E+0≪	4.741E+0	4.702E+0	4.715E+0	4.713E+0	4.713E+0
4	1.25	3	1.195E-3	1.010E-3	9.142E-4	1.612E+0	4.796E+0	1.690E+0	4.895E+0	1.476E+0≪	5.060E+0	5.187E+0	5.223E+0
5	1.50	3	1.891E-3	9.408E-5	7.523E-4	1.598E+0	4.768E+0	1.654E+0	4.825E+0	1.709E+0	4.884E+0	1.755E+0≪	4.951E+0
6	2.00	3	1.631E-2	8.931E-3	6.151E-3	1.601E+0	4.775E+0	1.663E+0	4.838E+0	1.724E+0	4.902E+0	1.783E+0	4.970E+0
7	1.01	5	9.327E-5	8.278E-5	7.448E-5	1.568E+0	4.706E+0≪	1.595E+0	1.650E+0	1.670E+0	1.691E+0	1.712E+0	1.734E+0
8	1.10	5	8.502E-5	7.264E-5	6.496E-5	1.573E+0	4.717E+0	1.579E+0	4.722E+0	1.589E+0≪	4.719E+0	4.709E+0	4.713E+0
9	1.25	5	3.442E-5	3.623E-4	1.953E-4	1.558E+0	4.688E+0	1.534E+0	4.662E+0	1.513E+0	4.627E+0	1.508E+0	3.647E+0≪
10	1.50	5	6.756E-3	2.938E-3	2.039E-3	1.590E+0	4.751E+0	1.628E+0	4.790E+0	1.666E+0	4.830E+0	1.701E+0	4.875E+0
11	2.00	5	4.810E-2	3.338E-2	2.355E-2	1.576E+0	4.723E+0	1.587E+0	4.734E+0	1.597E+0	4.745E+0	1.608E+0	4.756E+0
12	1.01	10	3.004E-4	2.616E-4	2.303E-4	1.562E+0	4.694E+0≪	1.557E+0	1.570E+0	1.569E+0	1.569E+0	1.569E+0	1.569E+0
13	1.10	10	1.880E-4	2.438E-4	1.942E-4	1.560E+0	4.692E+0	1.540E+0	4.670E+0	1.525E+0	4.618E+0≪	1.537E+0	1.600E+0
14	1.25	10	5.107E-3	2.079E-3	1.432E-3	1.585E+0	4.743E+0	1.616E+0	4.774E+0	1.645E+0	4.806E+0	1.670E+0	4.846E+0
15	1.50	10	3.691E-2	2.535E-2	1.668E-2	1.552E+0	4.674E+0	1.514E+0	4.636E+0	1.477E+0	4.599E+0	1.439E+0	4.560E+0
16	2.00	10	1.160E-1	9.366E-2	7.602E-2	1.555E+0	4.678E+0	1.520E+0	4.645E+0	1.487E+0	4.612E+0	1.454E+0	4.578E+0
17	1.01	20	9.700E-4	7.264E-4	5.210E-4	1.527E+0	4.628E+0≪	1.423E+0	1.353E+0	1.302E+0	1.247E+0	1.193E+0	1.139E+0
18	1.10	20	7.116E-4	1.317E-3	2.749E-4	1.521E+0	4.613E+0	1.422E+0	4.513E+0	1.324E+0	4.409E+0	1.231E+0	4.265E+0≪
19	1.25	20	3.009E-2	2.051E-2	1.284E-2	1.542E+0	4.655E+0	1.486E+0	4.599E+0	1.430E+0	4.541E+0	1.375E+0	4.483E+0
20	1.50	20	9.038E-2	7.240E-2	5.635E-2	1.512E+0	4.594E+0	1.394E+0	4.476E+0	1.276E+0	4.358E+0	1.159E+0	4.240E+0
21	2.00	20	1.521E-1	1.286E-1	1.163E-1	1.426E+0	4.423E+0	1.126E+0	4.123E+0	8.434E-1	3.813E+0	5.645E-1	3.509E+0
22	1.01	100	5.587E-4	5.447E-4	4.683E-4	1.547E+0	4.665E+0	1.503E+0	4.608E+0	1.482E+0≪	2.676E+0≪	1.534E+0	1.586E+0
23	1.10	100	7.291E-2	5.627E-2	4.397E-2	1.556E+0	4.684E+0	1.528E+0	4.656E+0	1.499E+0	4.628E+0	1.472E+0	4.602E+0
24	1.25	100	1.697E-1	1.529E-1	1.409E-1	1.579E+0	4.727E+0	1.588E+0	4.732E+0	1.603E+0	4.736E+0	1.587E+0	4.729E+0
25	1.50	100	2.214E-1	2.145E-1	2.084E-1	1.549E+0	4.671E+0	1.506E+0	4.634E+0	1.467E+0	4.599E+0	1.431E+0	4.564E+0
26	2.00	100	2.155E-1	2.057E-1	1.979E-1	1.503E+0	4.575E+0	1.365E+0	4.437E+0	1.236E+0	4.311E+0	1.096E+0	4.199E+0
27	sawtooth		1.223E-1	1.081E-1	9.672E-2	1.570E+0	4.712E+0	1.570E+0	4.712E+0	1.570E+0	4.712E+0	1.570E+0	4.712E+0

	X_0	m	ϕ_9	ϕ_{10}	ϕ_{21}	ϕ_{31}	ϕ_{41}	ϕ_{51}	ϕ_{61}	ϕ_{71}	ϕ_{81}	ϕ_{91}	ϕ_{101}
1	1.0001	3	8.760E-1	8.043E-1	4.633E+0	3.004E+0	1.378E+0	6.036E+0	4.413E+0	2.791E+0	1.170E+0	5.833E+0	4.218E+0
2	1.01	3	4.844E+0	4.859E+0	1.571E+0	3.342E-2	4.760E+0	3.203E+0	1.645E+0	8.769E-2	4.813E+0	3.255E+0	1.697E+0
3	1.10	3	4.713E+0	4.713E+0	1.570E+0	3.147E+0	≪4.686E+0≫	3.062E+0	1.491E+0	6.187E+0	4.603E+0	3.018E+0	1.433E+0
4	1.25	3	5.296E+0	5.358E+0	1.572E+0	3.137E+0	4.730E+0	5.982E+0	1.670E+0≫	≪1.857E-1	4.893E+0	3.354E+0	1.804E+0
5	1.50	3	5.251E+0	5.029E+0	1.570E+0	3.141E+0	4.713E+0	6.281E+0	1.574E+0	3.129E+0	4.726E+0	3.427E+0	1.606E+0
6	2.00	3	1.834E+0≪	5.047E+0	1.571E+0	3.141E+0	4.714E+0	6.281E+0	1.575E+0	3.136E+0	4.722E+0	6.268E+0	1.596E+0
7	1.01	5	1.754E+0	1.775E+0	1.569E+0	≪3.173E+0≫	1.660E+0	1.111E-1	4.847E+0	3.300E+0	1.752E+0	2.051E-1	4.940E+0
8	1.10	5	4.712E+0	4.712E+0	1.570E+0	3.141E+0	4.711E+0	5.276E-3	≪1.561E+0≫	6.261E+0	4.691E+0	3.116E+0	1.543E+0
9	1.25	5	1.539E+0	1.592E+0	1.570E+0	3.141E+0	4.711E+0	3.068E-3	1.558E+0	3.163E+0≫	≪3.744E+0	7.739E-2	4.855E+0
10	1.50	5	1.725E+0	4.934E+0	1.571E+0	3.141E+0	4.713E+0	6.282E+0	1.573E+0	3.137E+0	4.721E+0	6.264E+0	1.599E+0
11	2.00	5	1.619E+0	4.767E+0	1.570E+0	3.141E+0	4.712E+0	6.283E+0	1.570E+0	3.141E+0	4.712E+0	6.282E+0	1.571E+0
12	1.01	10	1.569E+0	1.569E+0	1.569E+0	≪3.153E+0≫	1.603E+0	4.035E-2	4.761E+0	3.199E+0	1.636E+0	7.446E-2	4.795E+0
13	1.10	10	1.563E+0	1.573E+0	1.570E+0	3.141E+0	4.710E+0	5.078E-3	1.536E+0	≪3.179E+0≫	1.680E+0	8.344E-2	4.815E+0
14	1.25	10	1.677E+0	4.909E+0	1.571E+0	3.141E+0	4.713E+0	6.281E+0	1.574E+0	3.135E+0	4.725E+0	6.253E+0	1.615E+0
15	1.50	10	1.402E+0	4.522E+0	1.570E+0	3.141E+0	4.711E+0	4.580E-5	1.570E+0	3.141E+0	4.711E+0	1.039E-3	1.568E+0
16	2.00	10	1.420E+0	4.545E+0	1.568E+0	3.139E+0	4.708E+0	6.278E+0	1.565E+0	3.135E+0	4.705E+0	6.275E+0	1.562E+0
17	1.01	20	1.085E+0	1.031E+0	1.573E+0	≪3.124E+0≫	1.527E+0	6.232E+0	4.650E+0	3.069E+0	1.488E+0	6.190E+0	4.609E+0
18	1.10	20	1.149E+0	1.180E+0	1.570E+0	3.141E+0	4.711E+0	1.633E-3	1.565E+0	3.149E+0	4.661E+0	≪2.430E-2≫	4.817E+0
19	1.25	20	1.321E+0	4.423E+0	1.570E+0	3.141E+0	4.711E+0	3.636E-4	1.568E+0	3.142E+0	4.708E+0	3.817E-3	1.562E+0
20	1.50	20	1.042E+0	4.122E+0	1.568E+0	3.139E+0	4.709E+0	6.280E+0	1.566E+0	3.137E+0	4.706E+0	6.278E+0	1.563E+0
21	2.00	20	2.735E-1	3.225E+0	1.569E+0	3.129E+0	4.699E+0	6.275E+0	1.535E+0	3.142E+0	4.660E+0	6.280E+0	1.522E+0
22	1.01	100	1.565E+0	1.571E+0	1.569E+0	3.143E+0	4.701E+0	2.764E-2≫	≪5.957E+0	3.267E+0	1.772E+0	2.033E-1	4.945E+0
23	1.10	100	1.444E+0	4.575E+0	1.570E+0	3.140E+0	4.711E+0	6.281E+0	1.570E+0	3.140E+0	4.713E+0	6.281E+0	1.573E+0
24	1.25	100	1.690E+0	4.827E+0	1.567E+0	3.131E+0	4.695E+0	6.269E+0	1.539E+0	3.093E+0	4.656E+0	3.661E-2	1.593E+0
25	1.50	100	1.396E+0	4.528E+0	1.572E+0	3.140E+0	4.719E+0	3.120E-3	1.585E+0	3.151E+0	4.734E+0	1.721E-2	1.599E+0
26	2.00	100	9.628E-1	4.075E+0	1.568E+0	3.139E+0	4.706E+0	2.499E-3	1.573E+0	3.139E+0	4.739E+0	6.281E+0	1.608E+0
27	sawtooth		1.570E+0	4.712E+0	1.570E+0	3.141E+0	4.712E+0	1.041E-7	1.570E+0	3.141E+0	4.712E+0	8.072E-7	1.570E+0

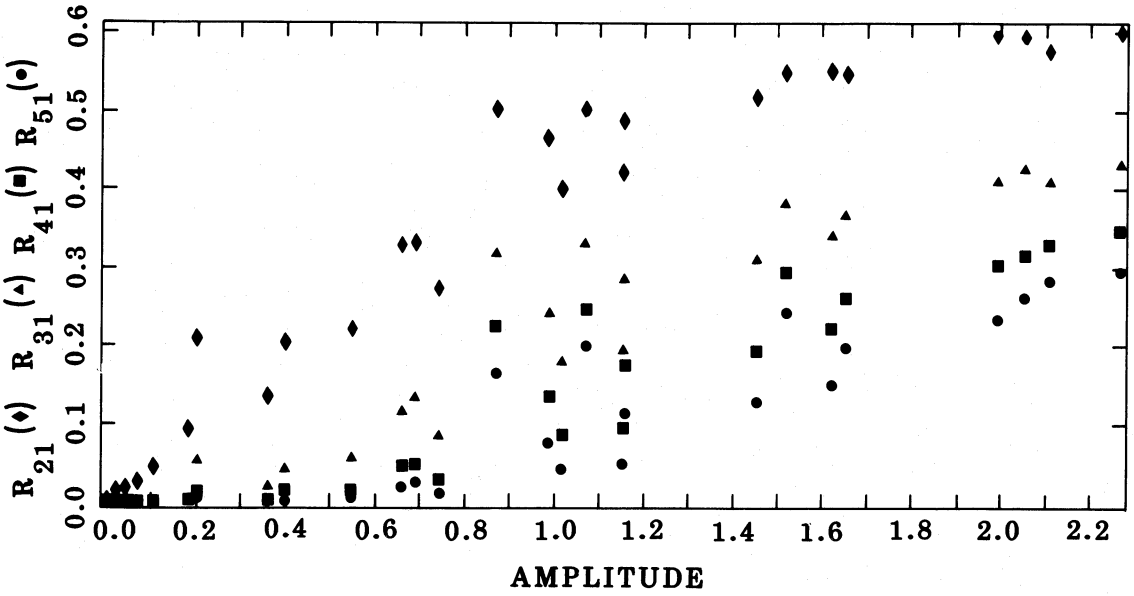

FIG. 2.—Relative Fourier amplitudes for harmonics 2–5 vs. total amplitude for the models in Table 1

Figures 4 and 5 show the same data plotted against skewness, and we see that very nice correlations are obtained.

This suggests that a direct comparison should be possible with the type ab RR Lyrae observations analyzed in detail by Petersen (1984), since for this group of stars skewness decreases linearly with increasing period and covers a range in skewness of 2–7, a range over which considerable variation is seen in the R calculated here. In fact, comparison of Petersen's Figures 4 and 5 with our Figures 4 and 5 shows remarkable agreement, both in the size of the R coefficients and in the shape of the variation as well: negative second derivative for R_{21}, R_{31}, and R_{41}; positive second derivative for R_{61} and R_{71}. Also, in both data sets R_{51} shows a nearly linear increase with increasing skewness. In all cases Petersen's R correlates better with skewness than with period, as in the one-zone results.

We conclude that only a very simple model is needed to understand the variations of the observed Fourier amplitudes and that the magnitude of each harmonic's amplitude relative to the fundamental is primarly a function of the skewness of the curve.

V. TRENDS IN PHASES

a) Specification of the Phase

We turn now to the trends in phases seen in the models. Recall that when comparing phases of different investigations, allowance must be made for type of analysis (sine or cosine), orientation of the curves ("light" or "velocity" orientation), and zero point of the phases (time origin). These considerations affect both the phases and the phase differences as defined by Simon and Lee (1981). We choose the "light curve" orientation here even though we are analyzing velocity curves, since this is the way the magnitude data are always displayed:

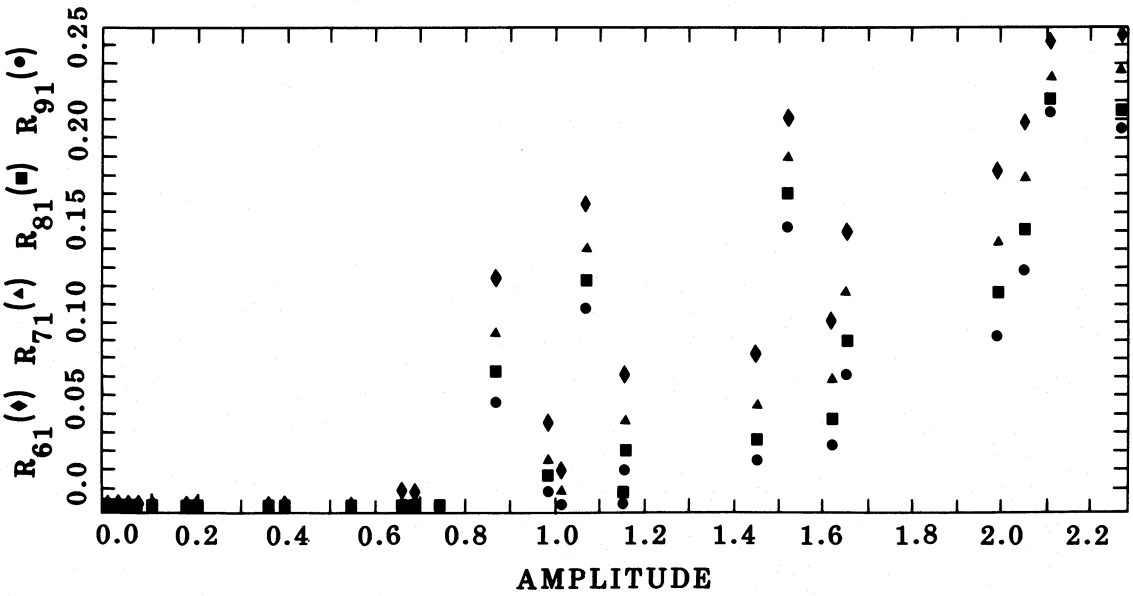

FIG. 3.—Relative Fourier amplitudes for harmonics 6–10 vs. total amplitude for the models in Table 1

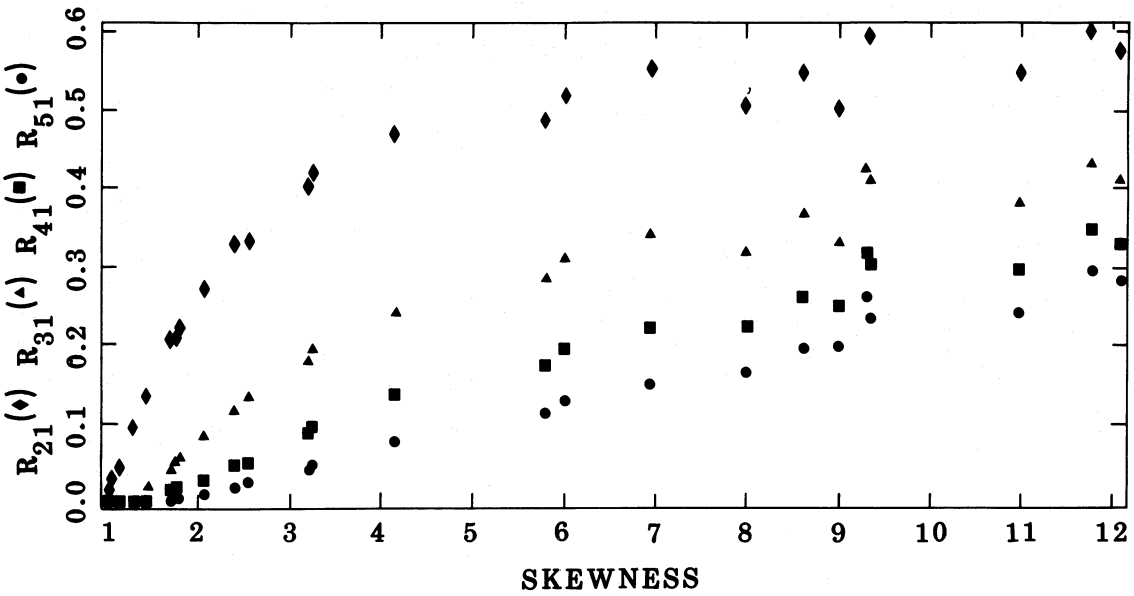

FIG. 4.—Relative Fourier amplitudes for harmonics 2–5 vs. skewness for the models in Table 1

"rising" branch is of shorter duration. The phase is chosen such that the midpoint of the rising branch is at phase 0.5. This preserves the symmetry of the curve to the fullest extent and avoids extraneous phase shifts caused by increasing skewness. The benefits of this choice will become apparent in the data analysis. See § VII*a* for a discusssion of the corrections required to compare data sets.

b) Results

Even a very quick examination of Table 1 suffices to show that these models simply do not show any gradual changes in the phases of the harmonics as a function of any parameter. With only a few exceptions, the phases ϕ_k are all one of two values: $\pi/2$ or $3\pi/2$. The ϕ_k represent unity minus the phase of the peak of the harmonic, so these values produce curves that cross the median point at phases 0 and 1 and thus preserve the nodes at these two limits. As we have seen, with smooth data, the least-squares fit is equivalent to a Fourier integral analysis, and the phase of each harmonic is independent of the others. Thus, in order to preserve the node, only these two phases are allowed. This requirement is relaxed for nonsymmetric light curves but probably applies to actual velocity curves. Of course, scatter in the observed points can also result in shifts in phases.

The pattern of these phases is readily apparent. For each model, the symbol " ≪ " appears among the ϕ_k: to the left of this symbol the phases alternate between the two values; to the right the phase is constant. The very low amplitude model (No. 1) shows nearly constant phases for all the harmonics, while the "sawtooth" model (No. 27) shows alternating phases

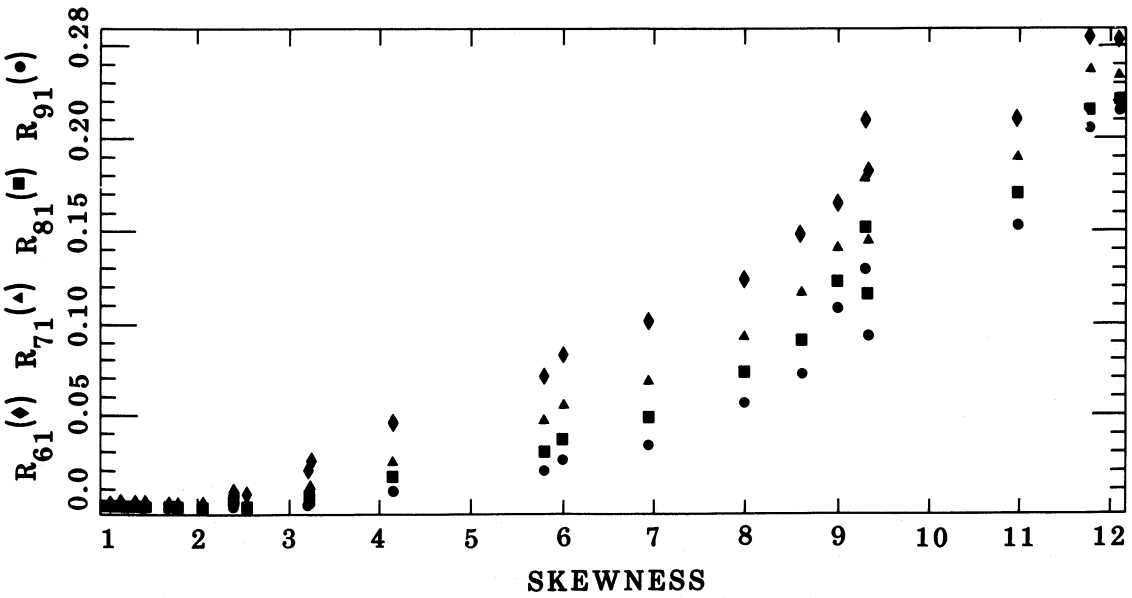

FIG. 5.—Relative Fourier amplitudes for harmonics 5–10 vs. skewness for ths models in Table 1

throughout the first 10 harmonics. The other models generally switch at some intermediate point, which depends primarily on their skewness. Figure 6 shows the value of the "switch" harmonic as a function of skewness: for curves above a skewness value of ~3.5 they show the "sawtooth" behavior through the tenth harmonic.

The pattern found in the relative phases (ϕ_{k1}) is somewhat different. Model No. 1 (nearly sinusoidal) shows a regular progression of phases in steps of $\pi/2$, increasing toward the lower harmonics. On the other hand, the sawtooth case (No. 27) also shows an identical progression, but now increasing toward higher harmonics, as indicated by arrows in Table 1. The other cases show a combination of both directions, with the switch occurring at a relative peak in phase, indicated by " $\ll \gg$ " or " $\gg \ll$ " in the table.

Comparing these two representations for the phases, we see that the switch points are comparable, although they are certainly much easier to spot in the raw ϕ_k than in the ϕ_{k1} data. In either case, several phases are needed to spot the pattern. The major difference between the two types of phases is that the relative phases sacrifice the lowest (and best determined) data point: the phase of the fundamental. It would certainly be an advantage to retain this data point in observational studies in which only a few harmonics are well determined. The extra effort required to achieve this is simply deciding on a standard zero point for the phases.

Reading down the phase columns from top to bottom gives some idea of the effect of varying the skewness: usually we find a sudden jump of magnitude π in a given ϕ_k or ϕ_{k1}. The jump occurs at very low values of the skewness for the lower harmonics, and higher values for the higher terms, as indicated by Figure 6.

c) *Comparison with Observations: ω Centauri*

In general, sets of actual stars do not show the type of constant-phase behavior seen here. Although this could be due in part to the effects of statistical scatter in the observed points and irregular choice of phase origin, trends are seen in the data that persist in the relative phases and undoubtedly represent some real effect in the stars. Simon and Lee (1981) suggest that these trends in Cepheids are caused by resonant interaction between different modes, a result strongly supported by the analytical analysis of Buchler and Kovacs (1985). If this hypothesis is correct, then such trends should not appear in the present models—only a single mode is permitted.

In this discussion we ignore the effects of color of observations, type of reduction process, etc., and concentrate on the corrections due to phase shifts and orientation of the curves as analyzed.

First, consider the observations of PG47. These calculations used intensity rather than magnitudes, and this gives the same orientation of the light curves as the present analysis (rising branch of shorter duration). The zero of phase is chosen to occur at maximum light. This choice introduces a deviation from the phases used above that is different in each case and cannot be corrected easily. Therefore, only the phase difference can be compared. Finally, the fit used in PG47 is a sum of sine terms rather than cosine terms. To correct for this, we apply a correction of $-\pi/2$ to all the PG47 phases and then compute the phase differences (this will change the phase differences by $[k-1]\pi/2$). The result of applying this procedure to the RR Lyrae type ab stars (Martin 1983, data) is shown in Figure 7, where phase differences have been plotted versus period, and the lines are regression lines for each phase difference. The trends are reasonably well defined, with some scatter for the higher harmonics. The RR Lyrae type c data are too few to see any trends in this data set.

These results should match those of Petersen (1984), who also analyzed the Martin (1938) mean curves of RR Lyraes in ω Cen. Petersen gives only phase differences, and data are given for only the lowest periods of type c a variables. In this case the magnitude data have been used in the analysis, so the curves need to be flipped to correspond to the convention used here. This is done by adding a correction of π to all the phases, implying a correction of $(k-1)\pi$ to the phase difference ϕ_{k1}. This means that every even-numbered phase differences (ϕ_{21}, ϕ_{41}, etc.) will be shifted by π, while the odd-numbered differences are unchanged. This is an important consideration, since

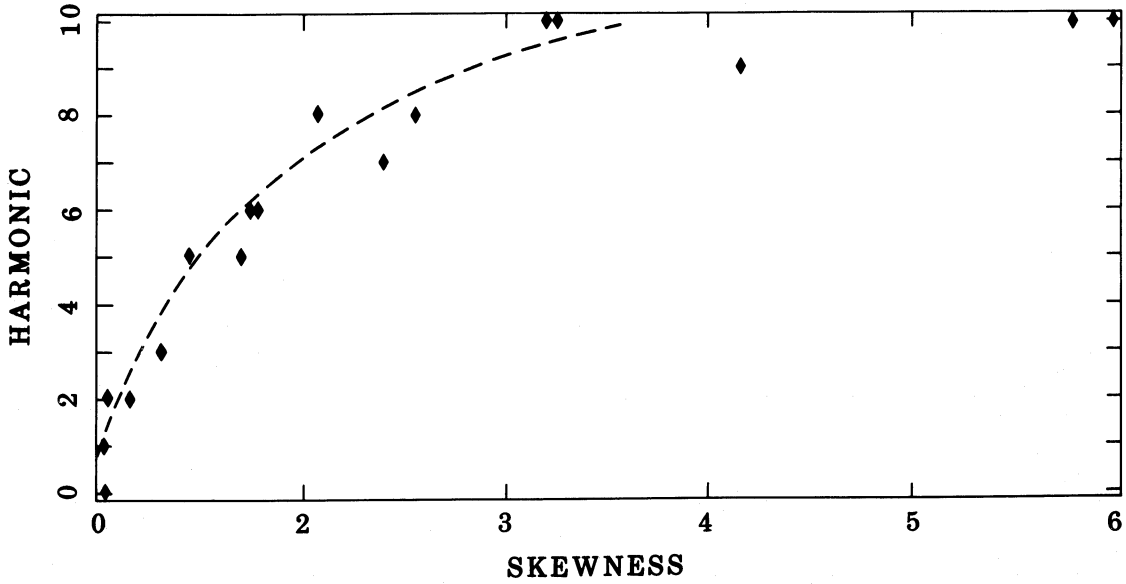

FIG. 6.—The harmonic number at which a switch from constant to alternating phases is expected. See text for details.

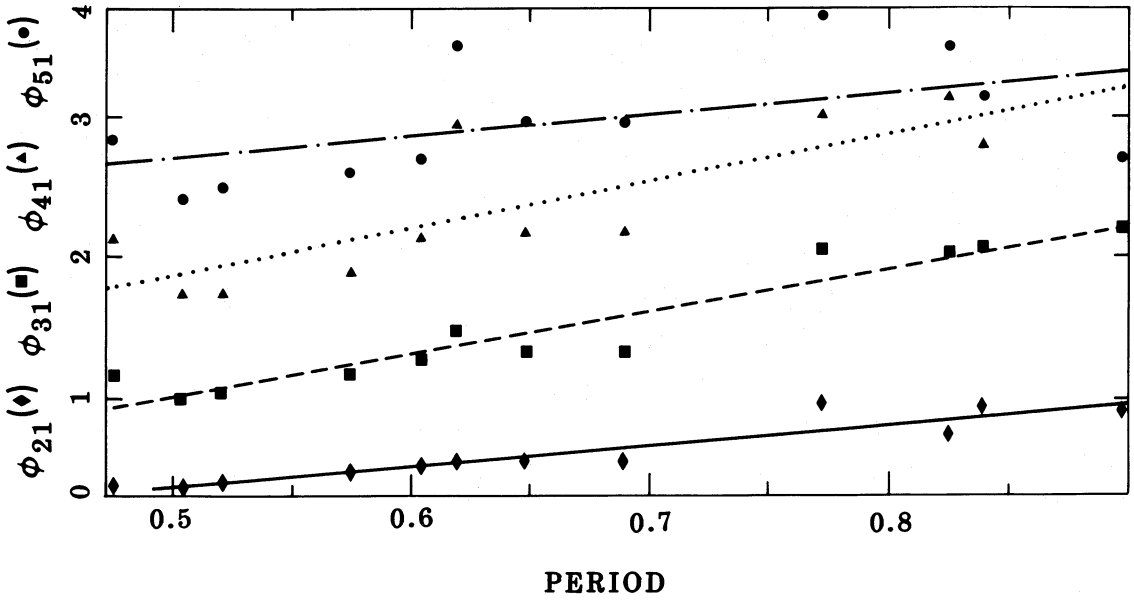

FIG. 7.—Phase differences for RR Lyrae type ab stars in ω Cen vs. period, as given by PG47. Regression lines are shown.

this is exactly the transformation that converts the "sinusoidal" phase progression found in the model data (descending phases) into the "sawtooth" progression (ascending phases). The transformed data, taken from Petersen's figures and data, are plotted as rough loci of the phase differences versus period in Figure 8*a*. Approximate values of the skewness are shown at the top of the figure. Figure 8*b* shows the complete data set of phase difference data, plotted now versus skewness. It is clear that, despite considerable scatter in the higher harmonics, smooth progressions, valid for both fundamental and first-overtone pulsators, emerge (the dashed lines are eye fits to the data). The conclusion is that a single easily determined parameter, the skewness of the light curve, seems to accurately predict all the phase difference data for these stars. Note the point at skewness 2.43 midway between the other ab and c cases in Figure 8*b*. This is variable 104, period of 0.868, with ϕ_{21} and ϕ_{31} exactly as predicted by the progression toward the c variables.

An important corollary to this result is that an overtone pulsator at an unusually high amplitude looks exactly like an ordinary fundamental pulsator, and vice versa, in the phase differences.

The phases in Figure 8 show the same progression as found in the PG47 data, and the values agree quite well. We expect the more sophisticated and more extensive analysis of Petersen to yield more accurate values than those of PG47.

As seen in Figure 8, the phase differences undergo progressive shifts in value as the period, or skewness, varies. These shifts are not found in the simple model. We knote, however, that the progression of phases found in the short-period type c variables and the long-period type b variables (both with skewness near 2), both match exactly the progression found in the "sawtooth" case in Table 1. This is the expected result, since, according to Figure 6, all phases through ϕ_{61} should show the sawtooth behavior for skewness greater than 2, and all phases through ϕ_{41} show this behavior for skewness greater than 1.3. This effect probably contributes to the scatter in the higher phases of Petersen's data, but the switch to sinusoidal behavior is not expected in the data as given and should be more apparent in the phases than in the phase differences.

It may be significant that the simple model prediction is seen at the two edges of the instability strip, and that the maximum deviation is found at the center of the strip. At the edges of the strip the pulsation is approximately a pure mode, while near the center the stars may be affected in some way by the proximity of the mode transition line: some influence of the other mode may, in fact, be emerging near the center of the strip.

Omega Cen is an interesting case in this respect, since in spite of vigorous searches by a number of workers (all unpublished at this time), not a single case of a mixed-mode RR Lyrae star has been found in this cluster. Harmonic analysis of clusters that do contain mixed-mode RR Lyrae stars, such as M3 or M15, would be of great interest, to see if any differences can be found.

It is interesting that although the values of the phases change, the nature of the progression (increasing phases with intervals of $\pi/2$ with increasing harmonics) tends to remain the same (the only exception is the short-period type a stars, where mode 3, 4, and 5 phases are crowded). This suggests that the only change is a shift in the fundamental phase relative to the other modes. It is imperative to examine the phases themselves in order to clarify this issue.

d) Comparison with Observations: Cepheids

The case of Cepheid light curves presents a somewhat different theoretical situation. All Cepheids are believed to be pulsating in the fundamental mode, so mode switching is not a consideration, except perhaps at the very shortest periods. Instead, a resonance at which the second overtone period is just twice the fundamental period is encountered at period roughly equal to 10 days (Simon and Schmidt 1976). This resonance is expected to affect the Fourier phases and thereby cause the progression in light curve shapes discussed by Hertzsprung (1926). Recently, SM85 have analyzed the data of Moffett and Barnes (1980, 1984), and these are the data dis-

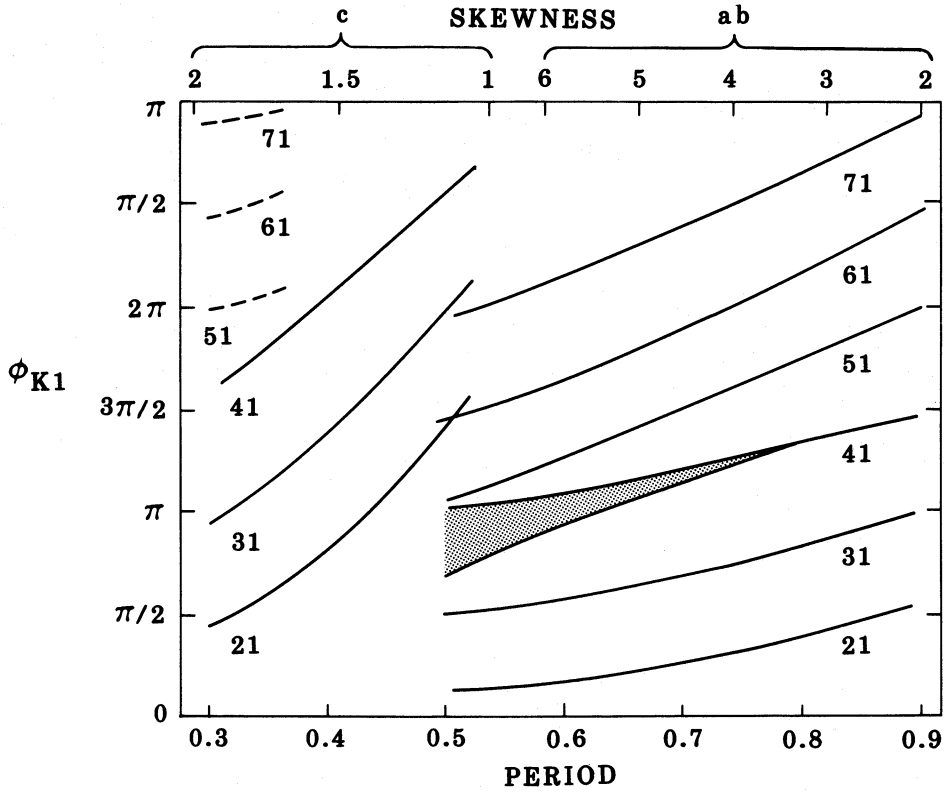

FIG. 8*a*

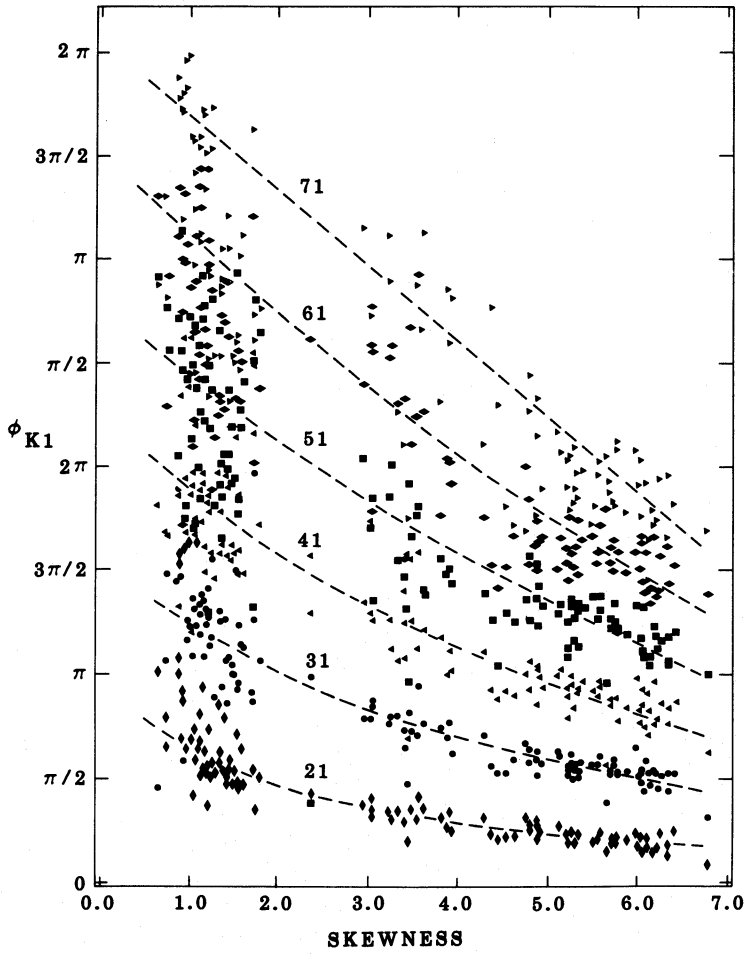

FIG. 8*b*

FIG. 8.—(*a*) Same as Fig. 7, but using the analyses of Petersen (1984) of Martin's (1983) ω Cen. data. Lines here represent trend lines in Petersen's figures. (*b*) plotted vs. skewness, showing Petersen data.

cussed here. In all cases, we choose the V magnitude data set as an example.

Although SM85 do not provide any data, some information can be obtained from their plots, but this limits the discussion to consideration of ϕ_{k1}. Figures 9, 10, and 11 are taken from Figures 1, 4, and 14 of SM85. The values of the phase differences have been adjusted exactly as in the Petersen data above, and all phases have been constrained to lie between 0 and 2π. The light lines show one possible interpretation of the data and are discussed below.

The scale of skewness in these figures is shown at the top: the stars with periods near 10 days show a early symmetrical light curve (although not sinusoidal), and the shorter as well as the longer periods show larger skewness. At low as well as high periods, a considerable scatter in amplitude is found, while at 7–10 days the amplitudes are more homogeneous (Fernie and Chan 1985). It is thus rather surprising that at exactly 8–10 day periods the maximum range in relative phases is found. It is impossible to tell in the ϕ_{21} plot whether the variation near 10 days is in the shape of a "cusp," as described by Simon, or a smooth change of a little over 2π in phase, as drawn in Figure 9. In the case of ϕ_{31}, Figure 10, however, it is clear that a smooth change is present, as is in the case of ϕ_{41}, Figure 11. In the large skewness limit of long periods, the values attained are very well defined: $\phi_{21} = \pi/2$, $\phi_{31} = \pi$, and $\phi_{41} = 3\pi/2$. These are exactly the values found in Table 1 for the "sawtooth" model, and in the RR Lyrae stars at both the longest and shortest periods. Indeed, the clump of Cepheids at period of ~ 5 days also show this progression, but the shortest period Cepheids deviate toward lower values (perhaps due to an incipient mode change to the overtone expected near a period of 2 days).

The ϕ_{41} plot shown as Figure 11 shows much the same trend as ϕ_{31}, with the exception that there appears to be a disjoint sequence of points at periods 6–8 days (*broken line*). This additional sequence is parallel to and displaced by $\pi/2$ from the main trend line, with a possible small group of stars near $\phi_{41} = \pi/2$ with a possible deviation of π from the main trend. This type of sudden jump in phase is just the type of behavior seen in the simple model. In fact, a jump in ϕ_{41} of π is expected for stars with small skewness, as is the case near periods of 10 days. The shape of the 10 day Cepheids is not sinusoidal, however, and this may account for the $\pi/2$ shift observed. In any case it would be of great interest to identify the light-curve characteristics, if any, that distinguish this small discrepant group of variables.

Returning to ϕ_{21}, Figure 9, we see the reason why the line has been drawn as shown. First, although the phase shifts seen here are larger than those of the RR Lyraes, the progression in phase is identical for the successive harmonics, so similar trends should be present in all the relative phases. Second, in the vicinity of 10 day periods, it is possible that a few stars may have skewness very close to unity and thus deviate by π from the main sequence, as seen in ϕ_{41}, and in model No. 1, Table 1.

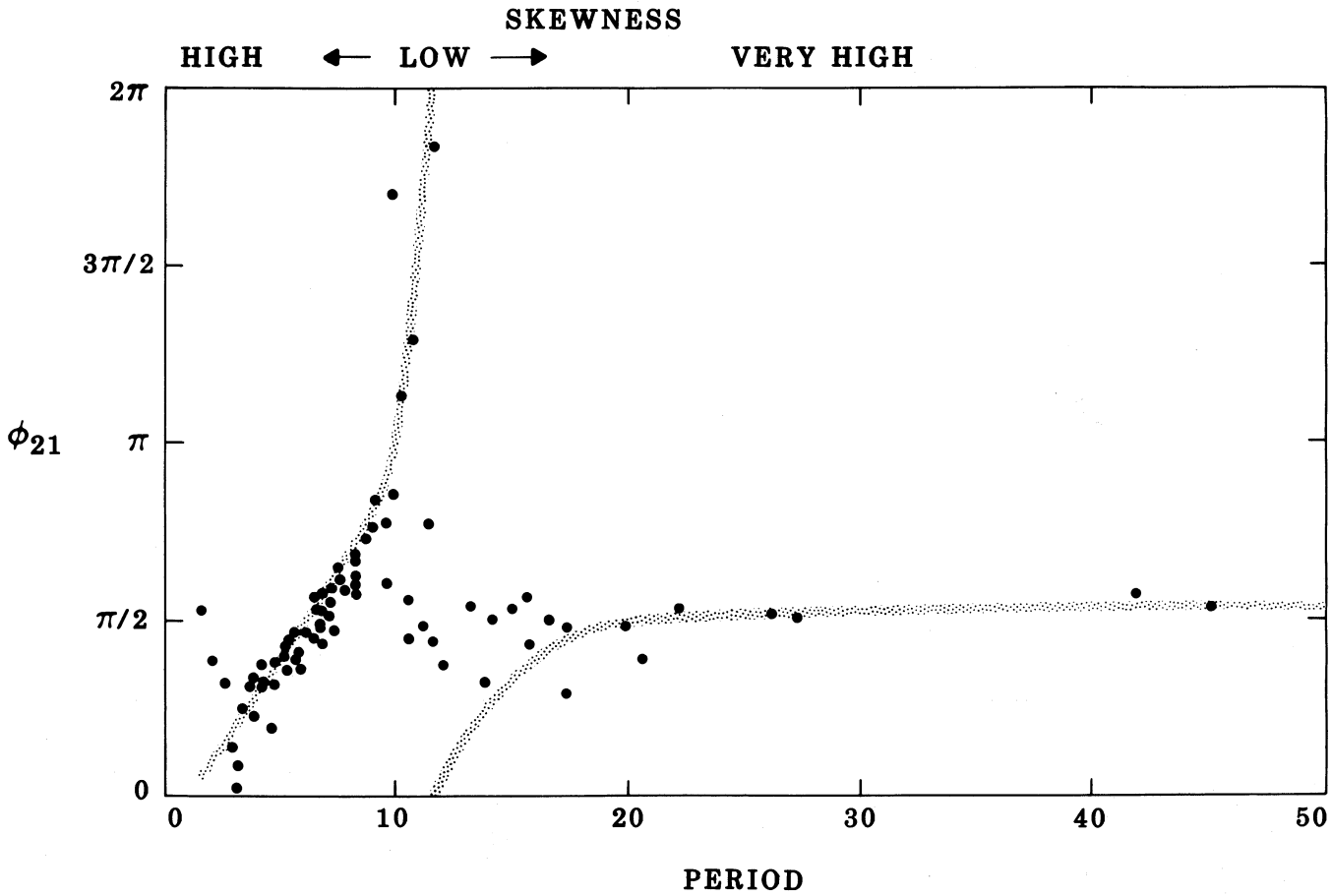

FIG. 9.—Phase difference ϕ_{21} vs. period as given by Simon and Moffett (1985). The line is a possible interpretation of the trend.

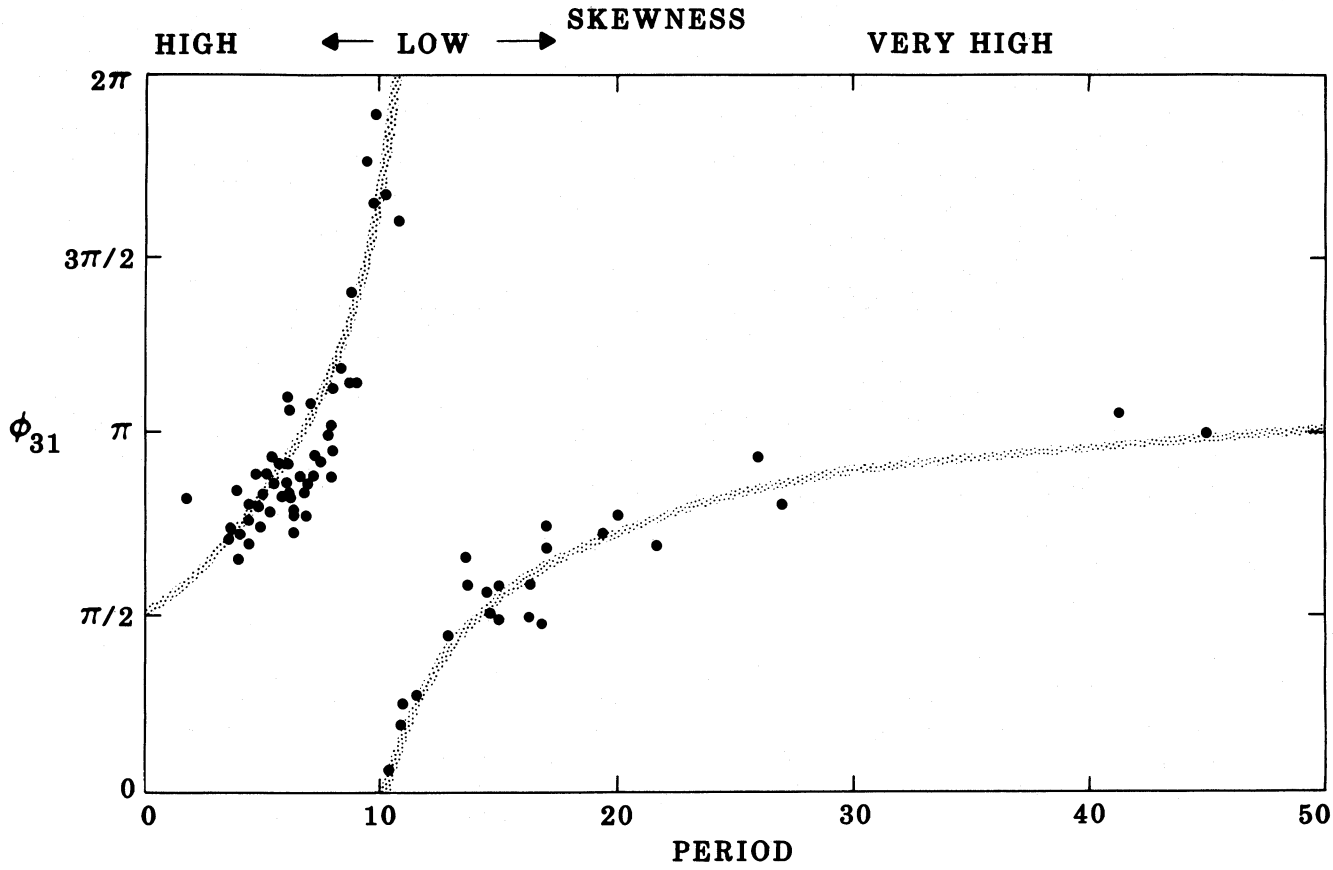

FIG. 10.—Sames as Fig. 9, for ϕ_{31}

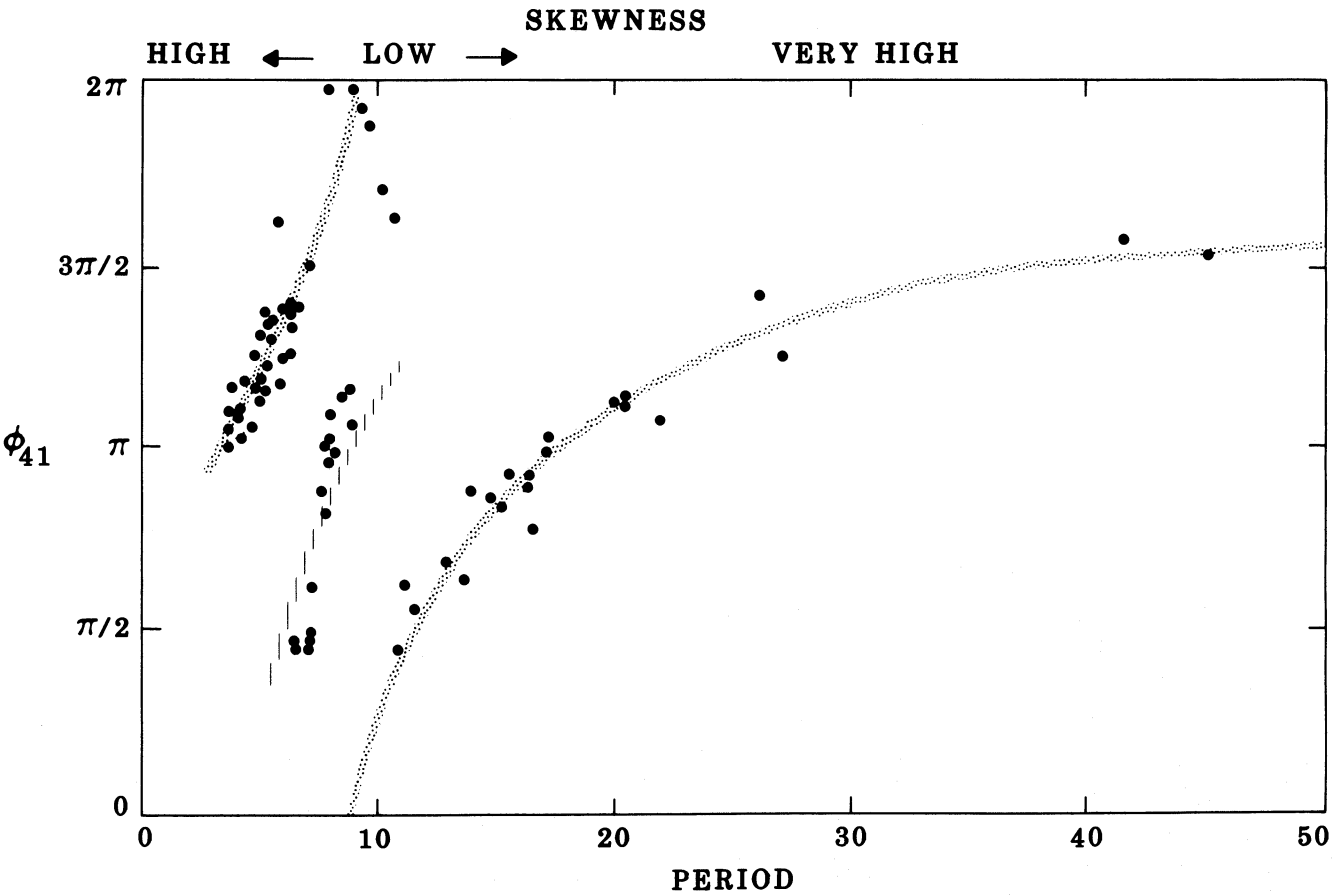

FIG. 11.—Same as Fig. 9, for ϕ_{41}

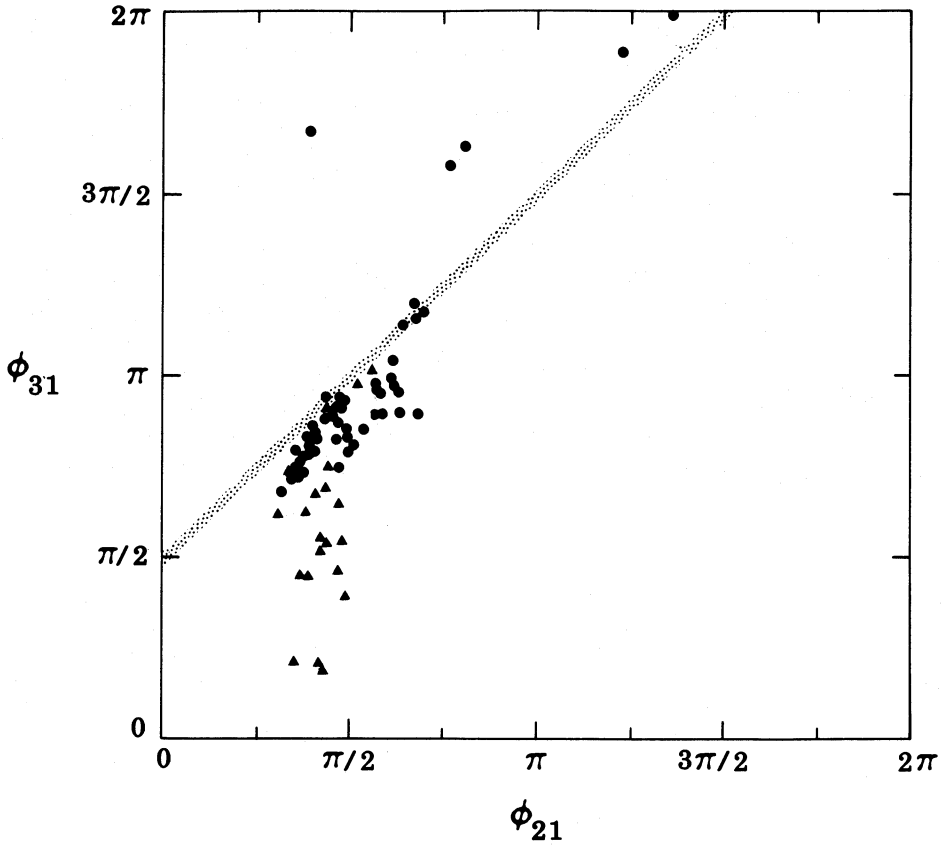

FIG. 12.—Phase-phase plot based on the data in Figs. 9 and 10. (Triangles denote stars with periods greater than 10 days.)

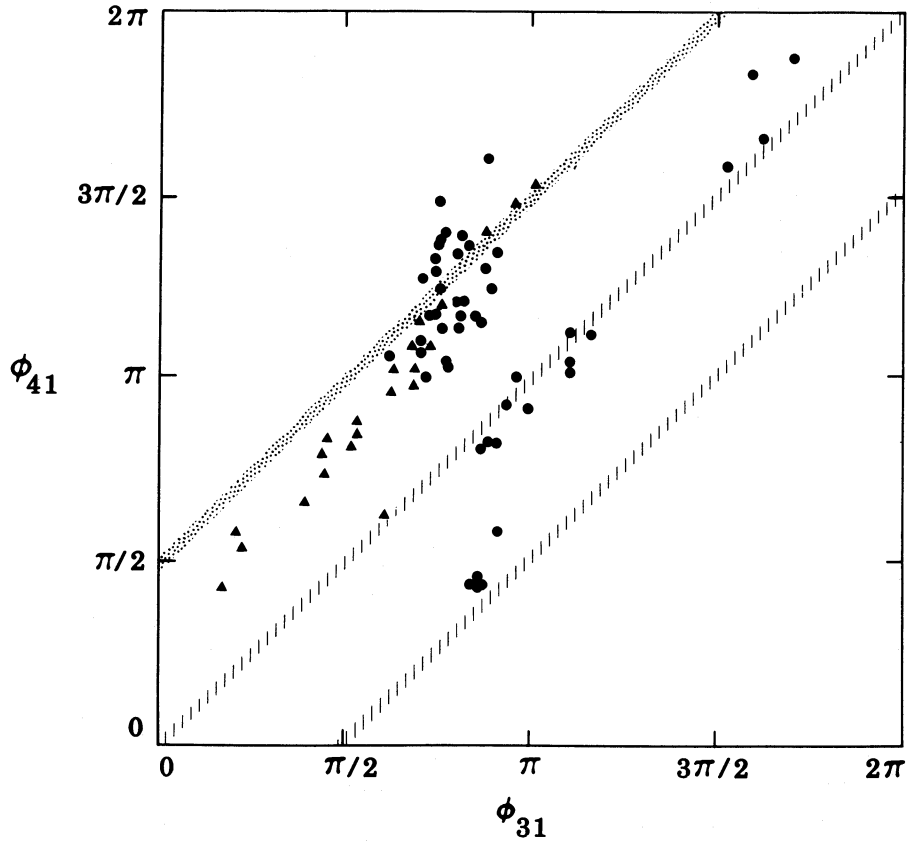

FIG. 13.—Phase-phase plot based on the data in Figs. 10 and 11. (Triangles denote stars with periods greater than 10 days.)

These stars could account for the points at $\phi_{21} = \pi/2$ near 10 days that seem to fill the gap between the two branches of the solid line.

As in the RR Lyrae case, the simple model fails to account for the drastic phase shifts seen in the SM85 plots. This is consistent with the resonance as driving these effects. We note that the behavior of the relative phases of Cepheids in the period range 3–10 days as a function of skewness is identical to that found for the RR Lyrae stars in ω Cen, as seen in Figure 8 (that is, varying from about $\phi_{21} = 0$ at large skewness to $3\pi/2$ for small skewness, and similar trends in the other phases). This is remarkable, since the resonance that presumably drives the variation in the Cepheids is lacking in the RR Lyrae stars. At longer periods, however, the variation of the phases in the Cepheids differs from that of the RR Lyrae stars, apparently increasing as the skewness increases, if the general trend is estimated correctly. This needs to be checked in the data.

SM85 also show several "phase-phase" plots, two of which we now reproduce here as Figures 12 and 13. Both plots have been converted to the convention used above (add π to the even phase differences) and plotted on a scale of 0 to 2π. Figure 12 shows ϕ_{31} versus ϕ_{21}; triangles denote stars with periods greater than 10 days, as in SM85. The line is the correlation obtained for a $\pi/2$ shift between these quantities. Most stars conform to this trend, the major exception being the stars with periods just greater than 10 days, whose ϕ_{21} is seen to be somewhat high, as noted above.

Figure 13 shows ϕ_{41} versus ϕ_{31} (the third combination is also plotted by SM85 but contains too much scatter to detect trends). In this plot the stippled line indicates the "simple" trend of $\pi/2$ shift and broken lines are shifted by $\pi/2$ and π from this line and show what seem to be the subsidiary sequences noted in Figure 11.

VI. BUMP TESTS

Whitney (1956) pointed out that the Cepheids in the period range of 7–10 days that show bumps could be represented reasonably well by a smooth light curve from which one cycle of a small-amplitude sine wave has been subtracted. Christy (1968) suggested that such a "bump" could be caused by an ingoing wave generated in the outer layers of a pulsating star that reflects from the stellar core and subsequently arrives at the surface. He showed that the dynamics of nonlinear pulsation models is consistent with this hypothesis and that the timing of such a reflected wave could account for the Hertzsprung progression seen in Cepheids.

Perhaps the effect of such a bump arriving at the surface at different phases could produce the type of phase shifts seen in variables. To test this idea a series of "bump" models were constructed. The bump itself was chosen to be one cycle of a sine wave with period 1/3 the fundamental period, amplitude 1/10 the total amplitude, and ten phases from 0 to 0.9. These choices were found to reproduce the Hertzsprung sequence reasonably well when applied to model 14: $m = 10$, $X_0 = 1.25$. The resulting models were analyzed, and the type of result is illustrated in Figures 14 and 15. These are "phase-phase" plots similar to Figures 12 and 13, but for the ten "bump" models with varying bump phase. We see that the result is an essentially random variation of the relative phases over a rather small range. The third harmonic did not track the small bump even though the periods matched. It appears that the simple reflected bump idea cannot explain the large phase changes observed. Of course, the actual effect of the reflected wave when it appears at the stellar surface is much more complicated than merely subtracting a simple sine wave at varying phases. A more reasonable test would employ a hydrodynamic model in which an outgoing wave is artificially generated deep in the interior.

VII. DISCUSSION

a) Methodology

The following procedure has been found to work well with both analytical and observational data sets:

1. Transform the data to a standard orientation. The orientation used here is obtained by analyzing the negative of observational magnitudes and velocities. It would be useful to display at least one curve in the orientation chosen to avoid ambiguity.
2. Compute a least-squares Fourier fit of the data.
3. Compute the mean curve given by the fit and determine the phase of the point at which the "rising" branch crosses the mean magnitude. Define this point as phase 0.5.

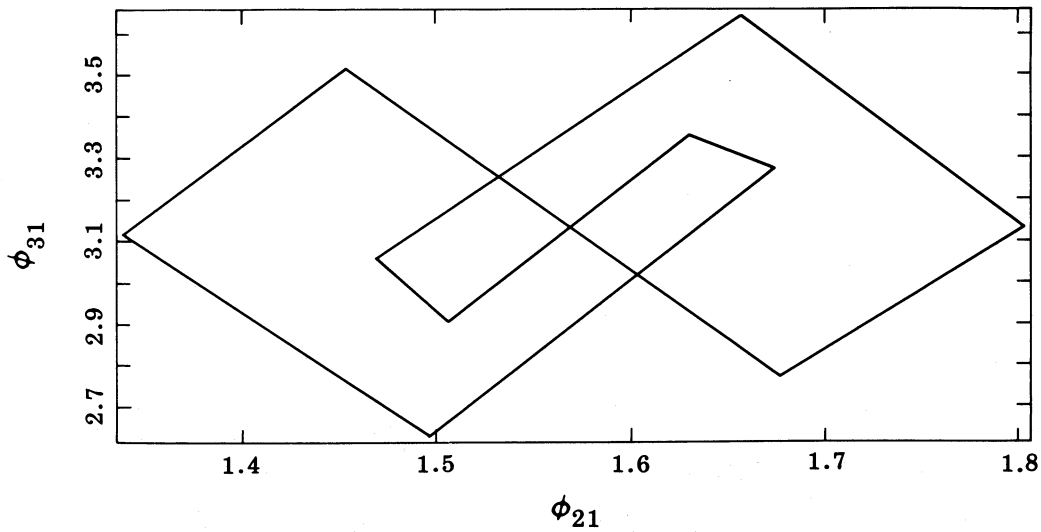

FIG. 14.—Phase-phase plot produced by adding a "bump" (see text) to model No. 14 at varying phases

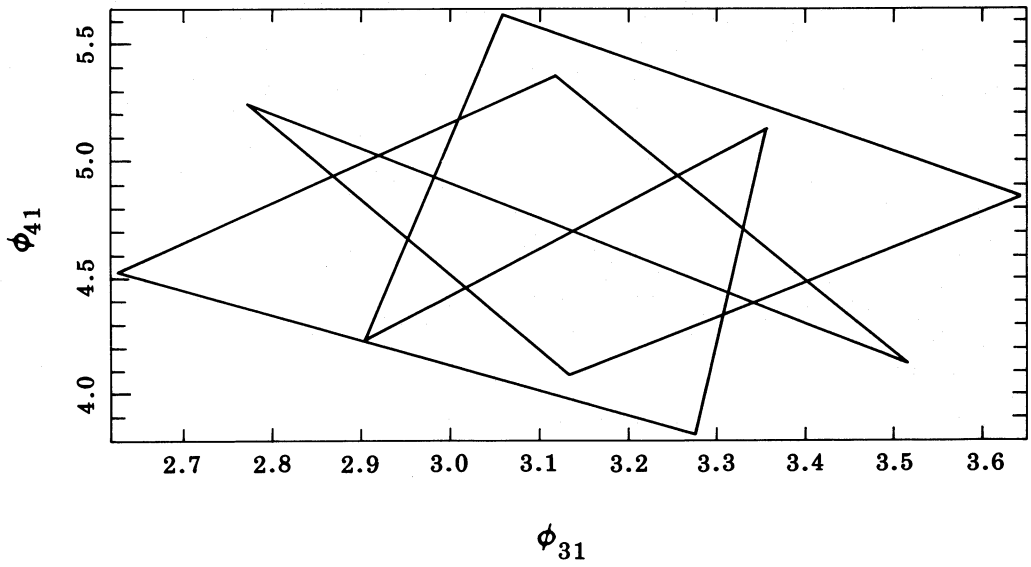

FIG. 15.—As in Fig. 14, for different phases

4. With analytical data, the Fourier phases can be transformed to the corrected phase origin, as described in § V. With observational data it is advisable to redo the Fourier fit with the new phases. Comparison with the transformed phases then gives a consistency check.

With this procedure, comparison of the Fourier phases between data sets is possible, and the most significant data point, ϕ_1, is retained. As seen in the model data and in PG47, trends in the phases are much cleaner than those in the phase differences.

b) *Results*

We have found that trends in the Fourier amplitudes of Cepheids and RR Lyrae stars can be reproduced by a simple one-zone model are primarily functions of the skewness of the curves, rather than amplitude. A major unsolved question is why stars at identical periods and amplitudes have a variety of light curve shapes.

We have seen that the Fourier phases of the model velocity curves are always one of two values ($\pi/2$ or $3\pi/2$), as determined by the nodes of the curves, and that the pattern of the phases in successive harmonics can be related to the skewness of the curve. Observed light curves also show this pattern but also show large shifts as a function of period of all the phases. It would be valuable to compare the model results to observed velocity curves rather than light curves, but the results are expected to be similar.

The observed phase shifts cannot be reproduced by simply adding a "bump" to the curves at varying phases. By their nature, we suggest that the observed shifts fall into two categories:

1. The very rapid variation of the phase differences in 9–11 day Cepheids of $\sim 2\pi$. This is probably a resonance effect.

2. The more gradual variation seen in 2–8 day Cepheids and in all RR Lyrae stars. These stars are far from any low-order resonance, so this effect may be due to an entirely different cause, such as an incipient mode switch. Of course, the possibility of other resonances in higher overtones should also be considered.

c) *Exhortation*

These results support the contention that Fourier parameters could be useful descriptors of variable star data. It is clear that their usefulness depends on building a large and reliable data base of light- and velocity-curve analyses. This can be done as large projects, such as those undertaken by Simon and Petersen, but equally valuable would be publication of the Fourier parameters obtained by routine fitting of observational data.

Fits should be taken to as high an order as possible. This is easily determined by computing fits to several different orders and picking the best one. Beyond some point, the fit will begin to be influenced by random fluctuations and gaps in the data. Analytic estimates of the accuracy of the fit parameters (Petersen 1984) are useful but could fail to detect wild fluctuation in a phase gap.

Studies are most useful if the data are published. Many of the trends seen in currently available data are not understood, and future studies will need complete data to allow progress. It is much better to publish the raw phases and amplitudes. Sophisticated functions of these can then be easily reconstructed, and allowance for new transformations must be made. If available, the amplitude and skewness of the curves should be given, as well as derived characteristics of the star.

The author wishes to thank Dr. N. Simon for a thorough review of the manuscript, and Dr. J. O. Petersen for providing a complete file of his ω Cen analyses. This project has been supported by NSF grant AST84-11029 through Mission Research Corporation.

REFERENCES

Bailey, S. I. 1902, *Harvard Ann.*, **38**, 132.
Baker, N. H. 1966, in *Stellar Evolution*, ed. R. F. Stein and A. G. W. Cameron (New York: Plenum), p. 333.
Buchler, J. R., and Kovacs, G. 1985, preprint. .
Fernie, J. D., and Chan, S. J. 1985, preprint.
Christy, R. F. 1968, *Quart. J.R.A.S.*, **9**, 13.
Hertzsprung, E. 1962, *Bull. Astr. Inst. Netherlands*, **3**, 115.
Klapp, J., Goupil, M.-J., and Buchler, J. R., 1985, *Ap. J.*, **296**, 514.

Kukarkin, B. W., and Parenago, P. P. 1937, *Astr. J. Soviet Union*, **14**, 186.
Madore, B. ed. 1985, *IAU Colloquium 82, Cepheids: Theory and Observations* (New York: Cambridge University Press).
Martin, W. C. 1938, *Leiden Annalen*, Vol. **17**, Part 2.
Moffett, T. J., and Barnes, T. G. 1980. *Ap. J. Suppl.*, **44**, 427.
———. 1984, *Ap. J. Suppl.*, **55**, 389.
Payne-Gaposchkin, C. 1947, *A.J.*, **52**, 218. (PG47).
Petersen, J. O. 1984, *Astr. Ap.*, **139**, 496.
———. 1985, *Copenhagen University Rept.*, No. 8.
Schaltenbrand, R., and Tammann, G. A. 1971, *Astr. Ap. Suppl.*, **4**, 265.
Simon, N. R. 1985, *Ap. J.*, **299**, 723.
Simon, N. R., and Davis, C. G. 1983, *Ap. J.*, **266**, 787.
Simon, N. R., and Lee, A. S. 1981, *Ap. J.*, **248**, 291.
Simon, N. R., and Moffett, T. J. 1985, preprint.
Simon, N. R., and Schmidt, E. G. 1976, *Ap. J.*, **205**, 162.
Simon, N. R., Teays, T. T. 1982, *Ap. J.*, **261**, 586.
Stellingwerf, R. F. 1972, *Astr. Ap.*, **21**, 91.
Whitney, C. A. 1956, *A. J.*, **61**, 192.

MARY DONOHOE and ROBERT F. STELLINGWERF: Mission Research Corporation, 1720 Randolph Road, SE, Alburquerque, NM 87106